

NASA TECHNICAL TRANSLATION

NASA TT F-12,276

INTERNAL OXIDATION OF NICKEL ALLOYS
CONTAINING A SMALL AMOUNT OF CHROMIUM

Shoji Goto,
Koji Nomaki,
Shigeyasu Koda

Translation of

Journal of the Japan Institute of Metals, 31, No. 4, pp. 600-606, 1967.

FACILITY FORM 602

N69-29389	
(ACCESSION NUMBER)	(THRU)
23	
(PAGES)	(CODE)
1	17
(NASA CR OR TMX OR AD NUMBER)	(CATEGORY)



NATIONAL AERONAUTICS AND SPACE ADMINISTRATION
WASHINGTON, D.C. 20546
JUNE 1969

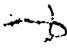
INTERNAL OXIDATION OF NICKEL ALLOYS CONTAINING A
SMALL AMOUNT OF CHROMIUM.

Journal of the Japan Shoji Goto[#]
Institute of Metals, Koji Nomaki^{**},
31, No.4, 600-606(1967). Shigeyasu Koda[#]

[#] The Research Institute for Iron, Steel, and Other
Metals, Tohoku University.

^{**} The Central Laboratory, Asahi Glass Co., Ltd.,
Yokohama.

Summary

 A dilute solid solution of nickel containing chromium up to 4 wt% in the form of a plate was internally oxidized at temperatures between 900° and 1300°C for various times in order to investigate the growth and structure of the subscale formed. The results obtained are as follows: (1) The relationship between the penetration depth of oxygen observed from the growth of the internally oxidized layer and the oxidation time of the alloys was well expressed by a parabolic law. It may be concluded that the activation process in internal oxidation is governed by diffusion of oxygen through the internally oxidized layer. (2) The activation energy for the growth of the internally oxidized layer decreased with increasing solute content in the alloys. (3) At high temperatures, the velocity

of internal oxidation increased, and the relation between the temperature T and the penetration depth E was expressed by $E \propto T^2$. (4) The penetration depth E increased with increasing oxygen pressure P_{O_2} in relation to $\log E \propto \log P_{O_2}$, and it was explained by Seybolt's law. (5) The higher the solute content, the more grain boundary diffusion prevailed. (6) Diffusion constants of oxygen in the internally oxidized layer were calculated by Wagner's equation. With increase of the Cr_2O_3 content, the diffusion constant of oxygen increased. This was explained by the interfacial diffusion of oxygen between the nickel matrix and the Cr_2O_3 particles. (7) From the results obtained above, the diffusion constant of oxygen in pure nickel was deduced.

(Received 22 November 1966.)

I. Introduction

With respect to the phenomenon of internal oxidation, even since this phenomenon was discovered by Rhines⁽¹⁾ in 1940, considerable research has been performed in the area of high temperature oxidation. For instance, there are studies of the internal oxidation in alloys where Al, Si, Cr, Ti, Mg, Be, and other metals have been added to Cu⁽²⁾, Ag⁽³⁾, or Fe⁽⁴⁾. With respect to the internal oxidation of the nickel alloys, Bonis and Grant⁽⁵⁾ have internally oxidized nickel alloys containing 1 wt.% Si, Al, Ti, or Cr at 700°-900°C, measuring the depth of the internal oxidation layer. Wolf and Evans⁽⁶⁾ also investigated the effect of oxygen pressure on the development of internal oxidation in Ni-Al alloys. On the other hand, alloys which have been made by the internal oxidation method have dispersed in their interior very fine stable particles of oxides, such that this has prompted a new area of study of dispersion-strengthened alloys⁽⁷⁾. From the standpoint of eventually making nickel dispersion-strengthened alloys, that is, internally oxidized alloys, the present investigation conducted internal oxidation of chromium-bearing nickel at temperatures of 900°-1300°C, and studied the effects of internal oxidation time, temperature, oxygen pressure, and solute concentration on the internal oxidation velocity. Also since the internal oxidation is due to diffusion of oxygen in the nickel, attention was also paid to the behaviour of the oxygen, and finally, the diffusion constant for oxygen in pure nickel was deduced.

II. Experimental Method

The raw materials used for the experiment consisted of better than 99.98% electrolytic nickel and chromium, better than 99.4%. Chemical analyses of the specimens are shown in Table 1.

Table 1 Chemical analysis of Ni-Cr specimens.

Cr content Specimen No.	wt% of Cr	vol% in Cr_2O_3
C	0.62	1.53
C 1	1.01	2.46
C 2	2.24	5.30
C 3	3.06	7.11
C 4	4.00	9.09

In the column where values are indicated in vol.%, this is the volume-% of Cr_2O_3 , into which all of the solute atoms are assumed to be internally oxidized.

The melting and casting of the specimens was performed with a high-frequency vacuum furnace. The ingots thus obtained were hot-forged, and homogenized by annealing for 24 hours at 1100°C in a vacuum, and then drawn down to 5mm diameter wire. This was further rolled to 3.5mm thickness, and then cut into 50mm lengths. The surface was then electrolytically polished in a solution of 50cc hydrogen peroxide and 200cc glacial acetic acid at 0°C and 1-2 amperes current, after which the specimens were annealed at 1100°C for 12 hours to relieve internal stress and to enlarge crystal size. The surfaces of the pieces were further electrolytically cleaned before being used for experimentation.

The method of internal oxidation consisted of a modification of the Rhines pack⁽¹⁾ method, that is, as shown in Figure 1, equal amounts of Ni powder and NiO powder were placed in the end of a silica tube, the sample was placed in the center of the tube, which was then sealed and evacuated. The tube was then heated in an electric furnace at 900°C - 1300°C for

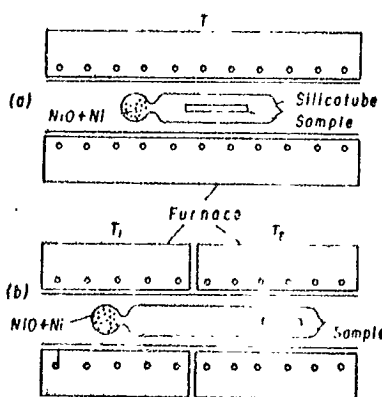


Fig.1 Experimental apparatus.

periods of 6, 12, 24, 48, and 72 hours with internal oxidation resulting from the oxygen released by the decomposition of the NiO. Also as shown in Figure 1(b), the temperatures of the oxygen supplying section and the sample were varied in order to vary the pressure of the oxygen being furnished for internal oxidation. After internal oxidation was completed, the tube was broken, the specimens were removed, a cross-section of the specimen buff-polished, and the depth of the internal oxidation layer was measured under an optical microscope.

III. Experimental Results

Photo 1(a) shows the structure of C1 as a result of internal oxidation at 1100°C . The deeper progression of internal oxidation with time can be clearly observed. In Figure 2 are shown the results of measurement of penetration depth with an optical microscope. It is seen that the depth of the oxidation layer increases parabolically with time, which characteristic has been reported previously in the case of internal oxidation of other alloys⁽⁸⁾.

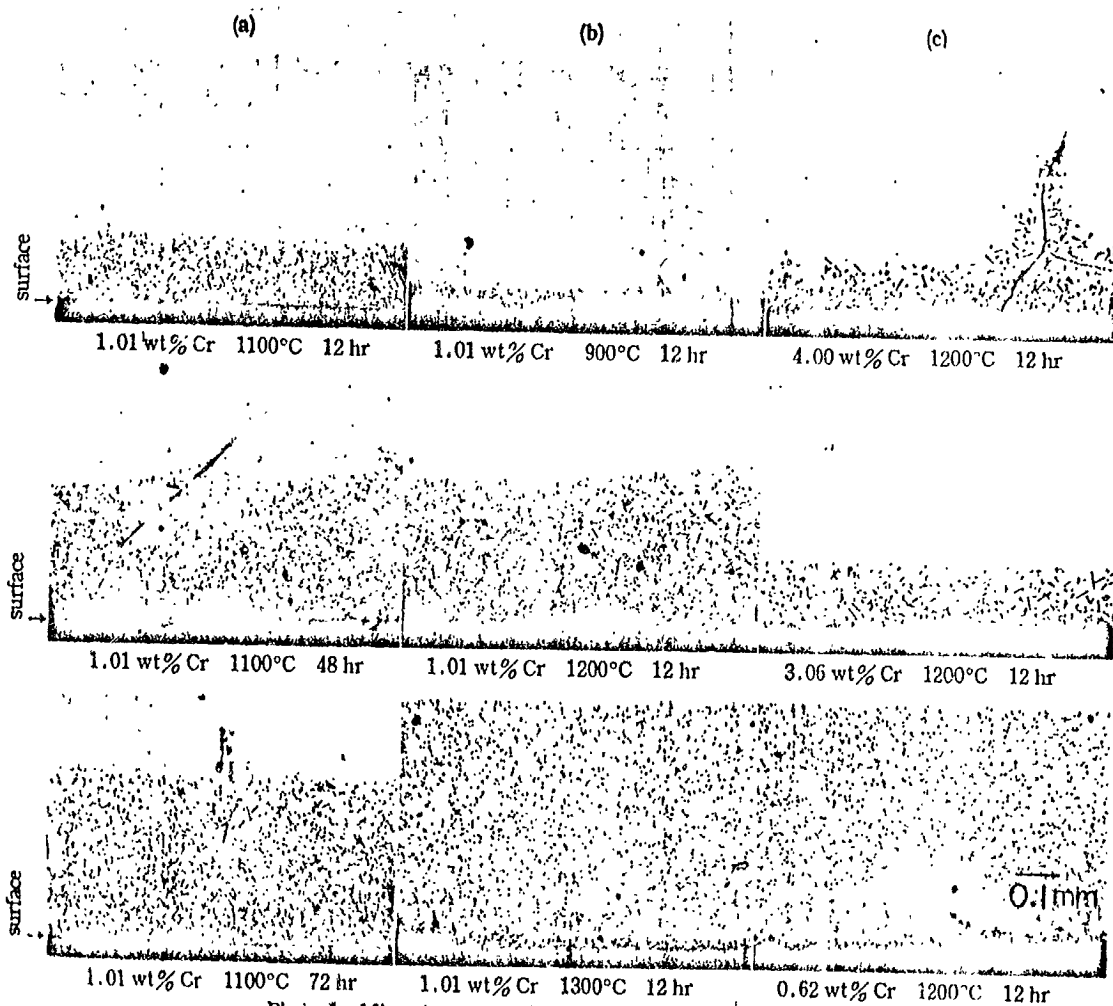


Photo.1 Microstructures of internally oxidized Ni-Cr alloys.

- (a) Microstructures of Ni-1.01 wt% Cr alloys internally oxidized for 12, 48 and 72 hr at 1100°C.
- (b) Microstructures of Ni-1.01 wt% Cr alloys internally oxidized for 12 hr at 900°, 1200° and 1300°C.
- (c) Microstructures of Ni-4.00 wt% Cr, Ni-3.06 wt% Cr, Ni-0.62 wt% Cr, internally oxidized for 12 hr at 1200°C.

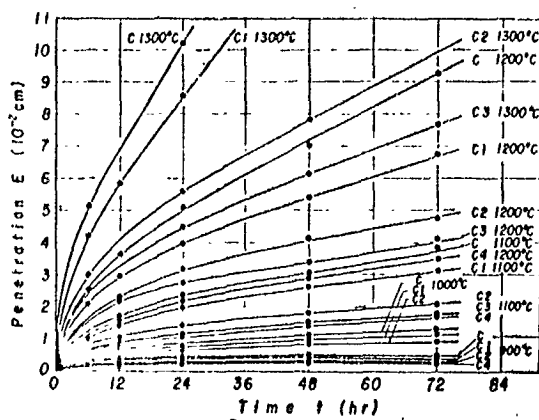


Fig. 2 Penetration depth E versus time t in internal oxidation.

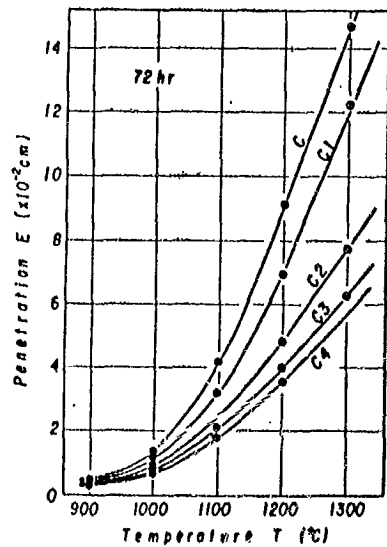


Fig. 3 Penetration depth E versus temperature T in internal oxidation.

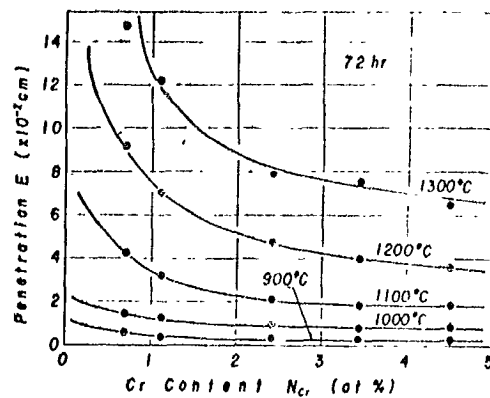


Fig. 4 Penetration depth E versus solute content N_{Cr} .

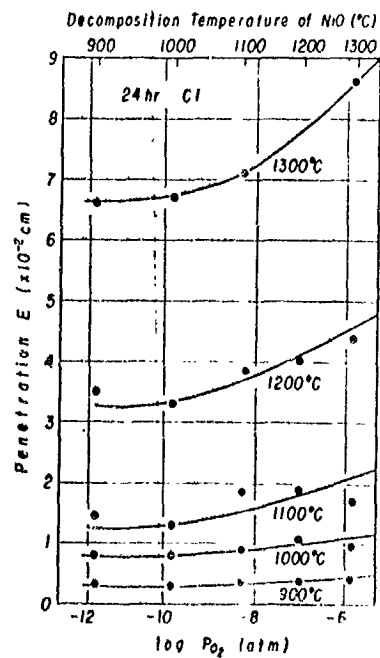


Fig. 5 Penetration depth E versus oxygen pressure P_{O_2} and decomposition temperature of NiO.

In Photo 1(b) is shown the result obtained with C1, where the temperature was varied for an internal oxidation time of 12 hours. It is seen that the internal oxidation layer grows rapidly with increasing temperature, and the parabolic relation in this case is shown in Figure 3. It is also seen that the temperature effect is stronger the smaller the concentration of the solute.

In Photo 1(c) is shown the structure of specimens with varying Cr content, the internal oxidation being performed at 1200°C for 12 hours. In sample C4, which has a high Cr content, the progress of internal oxidation by granular boundary diffusion can be noted. These relations are shown in Figure 4. It is seen that there is a tendency for the depth of the oxidation layer to decrease parabolically with an increase in the solute concentration. At the lower temperature of 900°C, the effect of solute content is not too evident, but the effect becomes more pronounced with higher Cr content.

In Figure 5 is shown the variation involved when the oxygen pressure required for internal oxidation gradually reaches the decomposition pressure of oxygen in NiO in the 900°-1300°C temperature range. From the curve for sample C1, which was internally oxidized at 1300°C for 24 hours, there is a tendency for the depth of the internal oxidation layer to increase parabolically with increasing oxygen pressure.

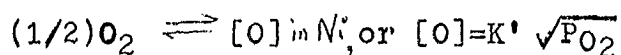
IV. Analysis of Experimental Results

1. Velocity of progression of internal oxidation layer

Internal oxidation is a preferred oxidation phenomenon occurring at high temperatures, and the following processes can be considered with respect to the development of the internal oxidation layer.

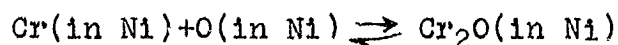
(a) Reaction, where oxygen gas, adsorbed at the surface of the alloy, becomes ionized and penetrates into the interior of the metal. (b) Reaction where the oxygen passes through the internal oxidation layer and diffuses to the oxidation front. (c) Reaction where the oxygen ion and the solute atom combine at the oxidation front to form an oxide. The velocity of propagation of the internal oxidation layer can be considered to be mainly governed by the slowest of these three processes.

If (a) is the controlling stage, then



where $[O]$ is the oxygen in solid solution, and K' is the equilibrium constant. Up to the solubility of the oxygen in the nickel, $[O]$ is proportional to the square root of the oxygen pressure, and therefore the velocity of internal oxidation is also proportional to $\sqrt{P_{O_2}}$. In the present experiment, the oxygen pressure was constant during the internal oxidation, and therefore, the depth E of the internal oxidation layer should increase linearly with time.

If (c) were the controlling stage, then



$$[Cr_2O_3] = K'' a_{Cr} \cdot a_O,$$

where K'' is the equilibrium constant, and a_{Cr} and a_O are respectively the activities of Cr and O in Ni. If one assumes then that the condition of the oxidation-front does not change, then at constant temperature, the reaction of oxide formation is constant, that is to say, the oxidation velocity is constant. In this case also, E becomes linearly related to time.

On the other hand, if (b) is the controlling stage, the oxygen ion diffuses through the metal according to the gradient of the concentration or proportional to $1/E$, and therefore, as is well known, the following parabolic relation applies.

$$E^2 = 2At = Kt \quad (1)$$

Here, A is a constant, t is time, and K is the velocity constant for the internal oxidation. Note that K depends on the condition of the internal oxidation layer, that is, as will be later described, it is proportional to $1/N_{Cr}$ at constant temperature, and proportional to E and D_O for constant Cr content. The curve in Figure 2 seems to match this parabolic law, and one therefore can conclude that (b) may be the controlling stage.

Now in attempting to determine K from the slope of the curves in Figure 6, one first notes that K may follow Arrhenius' formula, that is

$$K = B \exp(-Q/RT) \quad (2)$$

where B is a constant, Q is the activation energy necessary for the progression of internal oxidation, T is absolute temperature, and R is the gas constant.

Q can be determined from the relation between $\ln K$ and $1/T$, that is the slope of the curves in Figure 7, and the results are shown in Table 2. It is seen that there is a tendency for K and Q to decrease with increasing Cr content (N_{Cr}). The decrease of Q in this case is due to enhancement of oxygen diffusion by increased dispersed particle density which increases with N_{Cr} .

The decrease of K accompanying an increase in N_{Cr} is due to the decrease in Q, which means that although the oxygen is more easily diffusion N_{Cr} is larger than the oxygen which is supplied to the oxidation front, such that the cross section of capture of the oxygen atoms by the solute atoms increases, and together the progression of the internal oxidation layer is thus retarded.

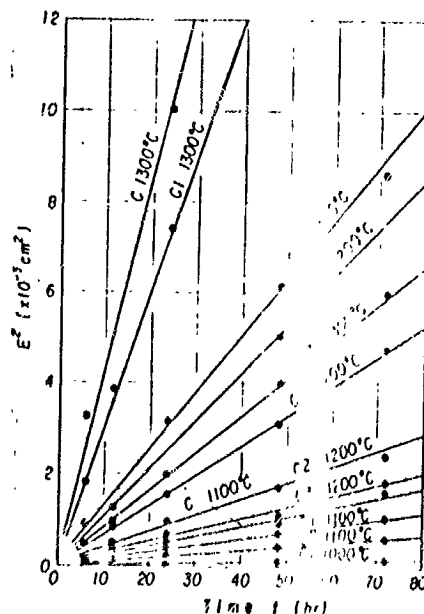


Fig.6 Some typical plots for square of penetration depth E versus time t of internal oxidation.

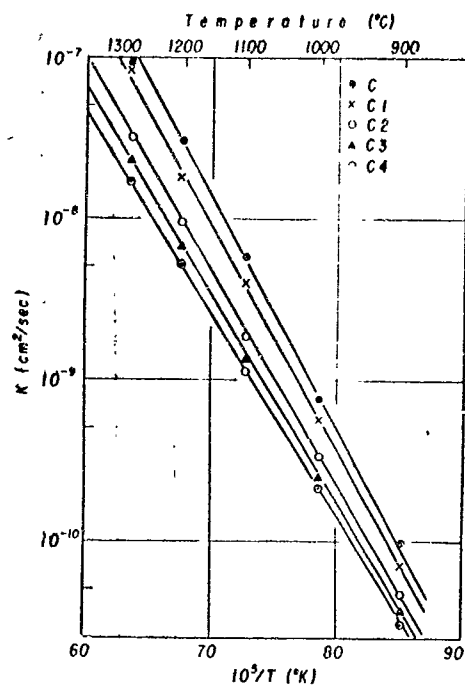


Fig.7 Logarithmic plot of the internal oxidation velocity constant K versus reciprocal of the absolute temperature T .

Table 2 Activation energy Q for growth of the internally oxidized layer in Ni-Cr alloys.

N_{Cr}	0.7	1.14	2.42	3.44	4.49
Q	at% Cr	at% Cr	at% Cr	at% Cr	at% Cr
kcal/mol	69	66	63	61	60

2. Dispersion of oxygen in the dispersion layer

According to Wagner⁽⁹⁾, the development of the internal oxidation layer depends strongly on the dispersion of the oxygen, and E can therefore be expressed in the following form.

$$E = 2 \gamma (D_0 t)^{1/2} \quad (3)$$

Here, γ is a constant, D_0 is the dispersion constant for oxygen in an isotropic dispersion layer. Wagner considered a density distribution such as shown in Figure 8, and using Fick's dispersion formula, and considering the diffusion to the oxidation front of the oxygen in solid solution in the dispersion layer and the solute atoms,

$$N_0 = N_0^{(s)} \{1 - \operatorname{erf}[x/2(D_0 t)^{1/2}] / \operatorname{erf} r\} \quad (4)$$

$$N_M = N_M^{(s)} \{1 - \operatorname{erf}[x/2(D_M t)^{1/2}] / \operatorname{erf}(r\varphi)^{1/2}\} \quad (5)$$

Here, x is the distance from the surface of the specimen, N_0 and N_M are respectively the densities of oxygen and solute atoms at distance x , $N_0^{(s)}$ is the oxygen density in the surface layer, $N_M^{(s)}$ is the solute density prior to internal oxidation, which corresponds to N_{C_1} in the present experiment. D_M is the dispersion constant for the solute atom. One also has

$$\varphi = D_0 / D_M \quad (6)$$

Let us now assume that just the proper amount of oxygen and solute atoms have flowed into the oxidation front to form an oxide, then,

$$\lim_{t \rightarrow 0} [-D_0 (\partial N_0 / \partial x)_{x=E-t}] = \lim_{t \rightarrow 0} [\nu D_M (\partial N_M / \partial x)_{x=E+t}] \quad (7)$$

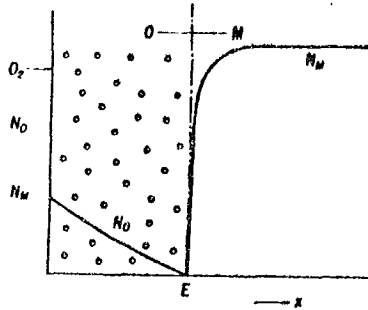


Fig.8 Schematic representation of Wagner's internal oxidation model.

Here, δ is an infinitesimal distance from E, ν is the mole ratio of the oxygen and the solute atom in the oxide, that is $\nu = O/M$. Then substituting (4) and (5) into (7), one has

$$N_0^{(s)} / \nu N_M^{(s)} = \exp(r^2) \operatorname{erf} r / \varphi^{1/2} \exp(r^2 \varphi) \operatorname{erf}(r \varphi^{1/2}) \quad (8)$$

If $\delta \ll 1$, $\delta \varphi^{1/2} \gg 1$, then approximately

$$\operatorname{erf} r \approx (2/\pi^{1/2}) r, \quad \exp(r^2) \approx 1 \quad (9)$$

$$\operatorname{erf} r \varphi^{1/2} \approx [\exp(-r^2 \varphi)] / \pi^{1/2} r \varphi^{1/2} \quad (10)$$

Furthermore, if (8), (9), and (10) are substituted into (3), one has

$$E = [2 N_0^{(s)} D_0 t / \nu N_M^{(s)}]^{1/2} \quad (11)$$

In any event, the above equation derived by Wagner neglects mechanisms (a) and (c), and assumes that there is always an amount of oxygen $N_O(s)$ at the surface, and that with the proper amount of oxygen and solute atoms for forming an oxide present, this oxidation takes place immediately, that is to say, that the oxygen diffusion process is the controlling mechanism.

As previously described, since oxygen diffusion was found to be the controlling stage in the experiment, our analysis proceeded on the basis of Wagner's formula, but first let us consider the validity of the condition

$\gamma \ll 1$, $\gamma \phi^{\frac{1}{2}} \gg 1$ in the present experiment.

For example, for specimen C1 in Figure 6, $K=4.0 \times 10^{-9}$ for 1100°C , and therefore $E^2=4.0 \times 10^{-9}t$. If one uses as an approximation the diffusion constant for oxygen in pure nickel obtained by Smithells et al.(10), $D_{O^{1100^\circ\text{C}}} = 2.4 \times 10^{-8} \text{ cm}^2/\text{sec}$, then from Equation (3), $(2\gamma)^2 = 4.0 \times 10^{-9} / 2.4 \times 10^{-8} = 4/24$, or $\gamma = \sqrt{1/24} \ll 1$. Also using Tyntrynik and Estulin's results(11), $D_{Cr^{1100^\circ\text{C}}} = 2.0 \times 10^{-11} \text{ cm}^2/\text{sec}$, one has $\gamma \phi^{\frac{1}{2}} = \gamma(D_O/D_M)^{\frac{1}{2}} = 50 \gg 1$.

Therefore, the conditions for deriving Equation (11) are sufficiently met.

On the other hand, from Equations (1) and (11), one has

$$D_0 = \nu N_M^{(a)} K / 2 N_0^{(a)} \quad (12)$$

Also, it was assumed at the beginning that the oxygen atoms diffused through an isotropic homogeneous dispersion layer, but as can be seen in Photo 2, there is considerable difference between the surface layer and the interior with respect to particle size and distribution.

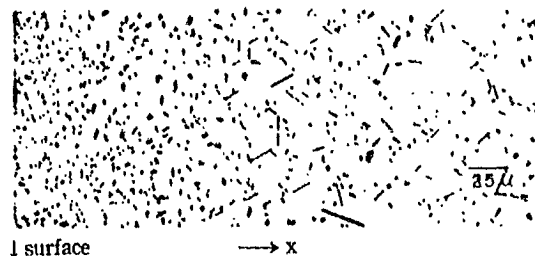


Photo.2 Microstructure of Ni-1.01wt%Cr alloy internally oxidized for 24 hr at 1100°C .

We shall neglect such differences here however, and attempt to calculate D_0 in Equation (12). Here, we take $\nu = 3/2$ since Cr_2O_3 is the oxide being formed, and the oxygen solubility limit will be taken for NiO (s) (12). The values thus obtained are shown in Figure 9. Note that normally Cr_2O_3 density should be the abscissa, but the Cr content was taken since this does not change the point of intersection with the abscissa, and the general character of the graph is not changed although there is a slight change in the slope of the curves. It is seen that D_0 increases with Cr content, that is, with particle density, the dependence being more pronounced at the lower temperatures. If D_0 were independent of particle density, the curves in Figure 9 should be parallel to the abscissa axis for all temperatures, but since D_0 is particle density dependent, let us divide the internal oxidation layer into the pure nickel region and the particle region, and let the activation energies for diffusion through these two regions be respectively Q_1 and Q_2 , then

$$D_0 = A \exp(-Q_1/RT) + B(T, N_{\text{Cr}_2\text{O}_3}) \exp(-Q_2/RT)$$

It can be seen that D_0 can be expressed as the sum of the first term, representing the diffusion of oxygen in pure nickel, and the second term, which is dependent on particle density.

It is also seen that in internal oxidation, grain boundary diffusion is active at lower temperatures (13) and with higher solute densities. In Figure 9, this stronger dependence of D_0 on N_{Cr} at lower temperatures can be observed. From these facts, it would seem that the larger the number of diffused particles, the larger the number of incoherent boundaries between the particles and the parent phase, and since these boundary surfaces act the same as grain boundaries, D_0 naturally becomes more strongly dependent on N_{Cr} (particle density) at the lower temperatures. At the higher temperatures, however, grain boundary diffusion is no longer effective in the diffusion of the oxygen, and since volume diffusion dominates, the dependence of D_0 on N_{Cr} tends to disappear. In other words, this seems to be the explanation for the independence of D_0 from Cr content in Figure 9 at temperatures above 1200°C . There are a few recent reports (2) concerning the enhancement of diffusion by the presence of diffused particles.

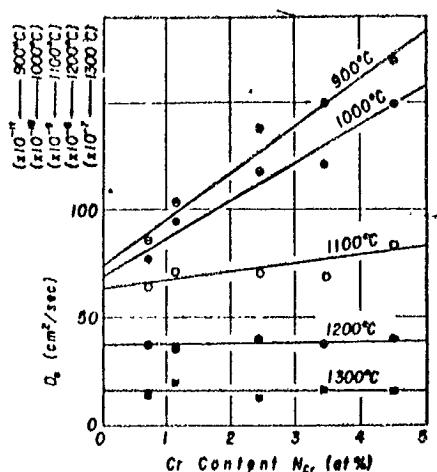


Fig.9 Effect of Cr content in Ni on the diffusion constant D_0 of oxygen in the internally oxidized layer.

The value of the diffusion constant extrapolated to Cr density zero can be considered as the diffusion constant for oxygen in pure nickel. These values are given in Table 3. The results by Smithells et al⁽¹⁰⁾ concerning the diffusion of oxygen in pure nickel are also listed for reference. It is seen that our experimental values are four to six times larger than their values.

Table 3 Diffusion constant D of oxygen in pure Ni.

T	The present investigation	T	Smithells & Ransley
900°C	7.4×10^{-10} cm ² /sec	900°C	1.5×10^{-10} cm ² /sec
1000°C	69×10^{-10} "	950°C	6.8×10^{-10} "
1100°C	63×10^{-10} "	1000°C	23.6×10^{-10} "
1200°C	37×10^{-10} "	1050°C	78.0×10^{-10} "
1300°C	16×10^{-10} "		

3. Oxygen diffusion activation energy

Using Arrhenius' formula, D_0 can be approximately expressed as follows.

$$D_0 = D \cdot \exp(-Q_0/RT)$$

Here, D^* is a constant, Q_0 is the activation energy for the diffusion of oxygen in the dispersion layer. From the slopes of the curves in Figure 10, Q_0 can be determined, and these values are given in Table 4.

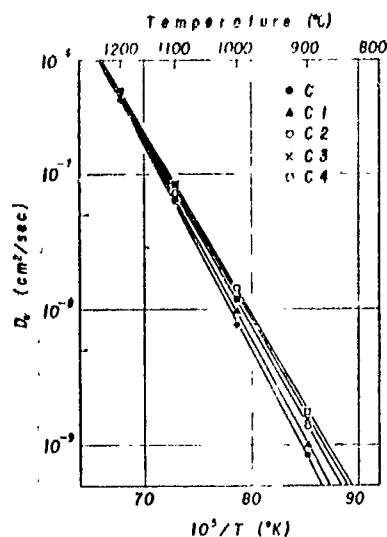


Fig.10 Diffusion constant D_0 of oxygen in the internally oxidized layer versus reciprocal of the absolute temperature T .

Table 4 Activation energy Q_0 for diffusion of oxygen in the internally oxidized layer.

Q_0 Cr%	0.70 at%	1.14 at%	2.42 at%	3.43 at%	4.49 at%
kcal/mol	68.8	66.1	62.9	61.0	60.6

Comparing this with the values of Q in Table 2, one finds that there is a good agreement. This agreement, that is a comparison of Q_0 , which was based on the assumption that diffusion of oxygen was the controlling process, and Q , which was obtained experimentally without any such assumption whatsoever, seems further proof for accepting the premise of the previously described (b) being the controlling process.

In Figure 11 are shown the activation energy values calculated similarly from the values of D in Table 3.

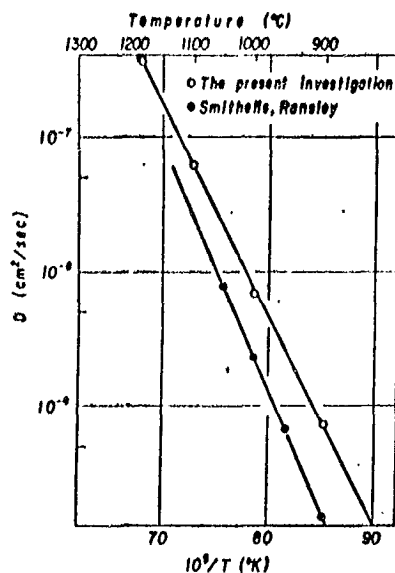


Fig.11 Diffusion constant D of oxygen in pure Ni versus reciprocal of the absolute temperature T .

It is seen that the diffusion constant for oxygen in pure nickel can be expressed as $D = 1.82 \times 10^{-4} \exp[-72000/RT]$, and that the activation energy is 72 kcal/mol.

The latter value is some 9 kcal/mol smaller than the 81.4 kcal/mol obtained by Smithell and others⁽¹⁰⁾. Messner et al⁽¹⁴⁾ report a self-diffusion activation energy of 69.7 kcal/mol for a simple nickel crystal. This value somewhat resembles the 72 kcal/mol figure obtained in our experiments, and it could be assumed that oxygen diffuses in nickel in a manner similar to the self-diffusion mechanism for nickel.

4. Effect of solute density on internal oxidation velocity

If internal oxidation occurs at constant temperature and for a fixed period of time, then from Equation (11), one obtains a relation between E and $N_M^{(s)}$, namely $E \propto 1/\sqrt{N_M^{(s)}}$. This expresses the relation already shown previously in Figure 4. This means that for a given amount of oxygen which has diffused to the oxidation-front, the collision probability for oxygen and the solute atoms increases only as the square root of $N_M^{(s)}$.

5. Effect of temperature on internal oxidation velocity

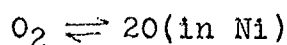
Let us consider an alloy with fixed solute density which has been internally oxidized for t hours. In this case, $D_0 = D \cdot \exp(-Q_0/RT)$, and $N_O^{(s)}$ varies as $N_O^{(s)} = XT + Y$ (X and Y are constants) in the temperature range 900°C-1300°C⁽¹²⁾, so that Equation (11) can be expressed in the following manner.

$$\ln E = (1/2) \ln [2(XT+Y)D^*/N_{Cr}^{(s)}] - Q_0/RT$$

The first term on the right is only weakly dependent on temperature so that $\ln E$ and $1/T$ are linearly dependent. When the data in Figure 3 is replotted in terms of $\ln E$ and $1/T$, this relation becomes quite evident. This means that the factor D_0 is mainly responsible for the temperature dependence of the internal oxidation velocity. The relation between E and D_0 is, from the above equation, $E^2 \propto D_0 \propto \exp(-Q_0/RT)$, in other words, the internal oxidation velocity increases exponentially with the temperature.

6. Effect of oxygen pressure on the internal oxidation velocity

Generally speaking, Seybolt's rule holds for the adsorption of gases by metals, that is,



$$\text{or } N_0 = \sqrt{k' P_{O_2}}$$

where $k' = (a_0)^2 / P_{O_2}$, and $a_0 = N_0$. Substituting this into Equation (11), one has

$$2 \ln E = \ln [2D_0 t \sqrt{k'} / N_{Cr}^{(s)}] + \frac{1}{2} \ln P_{O_2}$$

In Figure 5 in the current experiment, if the internal oxidation temperature is lower than the NiO decomposition temperature, for instance say the internal oxidation temperature is 1100°C but the NiO decomposition temperature is higher than 1100°C , there is some scattering of the data points. This is probably due to the fact that the oxygen pressure at the surface is higher than $N_0^{(s)}$, such that internal oxidation is occurring simultaneously with the oxidation of the parent nickel phase. On the other hand, when the internal oxidation temperature is lower than the NiO decomposition temperature, for instance if the internal oxidation temperature is 1300°C , then E is proportional to $\log P_{O_2}$ and it **increases parabolically**. If this relation is replotted in terms of $\ln P_{O_2}$ and $\ln E$, one has a linear relation, which agrees with the above derived formula. In any event, when the oxygen pressure is less than the solubility, Seybolt's rule holds and $\ln E$ is proportional to $\ln P_{O_2}$, since the oxygen molecules becomes atoms and dissolve in the nickel.

V. Conclusions

Nickel alloy bearing 0.62 to 4 wt% Cr was internally oxidized at temperatures of 900° to 1300°C, the progress observed, with the following results being obtained.

(1) The internal oxidation velocity varied parabolically with time. This meant that the diffusion of oxygen through the internal oxidation layer was the process controlling the progress of internal oxidation.

(2) The internal oxidation velocity increased with higher internal oxidation temperatures, the relation between the temperature T and the depth of the oxidation layer E being found to be $E \propto T^2$. This was considered to be due to the temperature dependence of the diffusion constant for oxygen in the internal oxidation layer.

(3) The internal oxidation velocity was larger for lower solute density $N_M(s)$, the relation being roughly $E \propto 1/\sqrt{N_M(s)}$. Also the internal oxidation velocity constant K and the activation energy Q were smaller for larger solute densities.

(4) The higher the solute atom density, the more significant was internal oxidation due to grain boundary diffusion.

(5) Using Wagner's formula $E = [2N_O(s)D_0t/\sqrt{N_M(s)}]^{1/2}$, when one calculates the diffusion constant D_0 of oxygen in the dispersion layer from the internal oxidation velocity constant K , one finds that the diffusion constant is large for high dispersed particle density, and that this trend is more pronounced at lower internal oxidation temperatures. This is assumed to be due to the fact that the boundary between the oxide particles and the parent metal phase tends to enhance diffusion.

(6) From the diffusion constant D_0 for oxygen in the dispersion layer, one can calculate the diffusion constant for oxygen in pure nickel. This is

$$D = 1.82 \times 10^4 \exp(-72000/RT) \text{ cm}^2/\text{sec}$$

(7) When the oxygen pressure is less than the solubility of oxygen in nickel, the depth of the internal oxidation layer increases with the oxygen pressure as $\log E \propto \log P_{O_2}$. This is assumed to be due to the fact Seybolt's rule holds with respect to the infusion of oxygen gas into the nickel.

REFERENCES

- (1) Rhines, F.N., Trans.AIME, 137, 246(1940).
- (2) For instance, Kimura and Watanabe, J.Japan Inst. Metals, 29, 885(1965).
- (3) For instance, Rapp, R.A., D.F.Frank, and J.V.Armitage, Acta.Met., 12, 505(1964).
- (4) For instance, Schenk, H., E.Schmidtman, and H.Müller, Arch.Eisenhütt., 31, 121(1960).
- (5) Bonis, L.J., and N.J.Grant, Trans.AIME, 224, 308(1962).
- (6) Wolf, J.S., and E.B.Evans, Corrosion, 18, 129(1962).
- (7) For instance, Komatsu, N. and N.J.Grant, Trans.AIME, 224, 705(1962).
- (8) For instance, Schwarzkopf, W.M., Z.Elektrochem., 63, 830(1959).
- (9) Wagner, C., Z.Elektrochem., 63, 772(1959).
- (10) Smithells, C.J. and C.E.Ransely, Proc.Roy.Soc., 55, 195(1936).
- (11) Tyntyunnik, A.D. and G.V.Estulin, Fizika, Metallov, Metallovedenie, 4, 558(1957).
- (12) Seybolt, A.V., Metals Handbook, Cleveland ASM, 1231(1948).
- (13) Goto and Koda, unpublished.
- (14) Messner, A., R.Benson, and J.E.Dorn, Trans.ASM, 53, 227(1961).